Contributions of Residue 45(CD3) and Heme-6-propionate to the Bimolecular and Geminate Recombination Reactions of Myoglobin†

Theodore E. Carver and John S. Olson*
Department of Biochemistry and Cell Biology, Rice University, Houston, Texas 77251
Stephen J. Smerdon, Szymon Krzywda, and Anthony J. Wilkinson
Department of Chemistry, University of York, York Y01 5DD, U.K.
Quentin H. Gibson and Richard S. Blackmore
Department of Biochemistry, Molecular and Cell Biology, Cornell University, Ithaca, New York 14853
J. Dezz Ropp and Stephen G. Sligar
Departments of Biochemistry and Chemistry, University of Illinois, Urbana, Illinois 61801
Received September 6, 1990; Revised Manuscript Received January 11, 1991

ABSTRACT: Overall association and dissociation rate constants were measured at 20 °C for O_2, CO, and alkyl isocyanide binding to position 45 (CD3) mutants of pig and sperm whale myoglobins and to sperm whale myoglobin reconstituted with protoheme IX dimethyl ester. In pig myoglobin, Lys^{45}(CD3) was replaced with Arg, His, Ser, and Glu; in sperm whale myoglobin, Arg^{45}(CD3) was replaced with Ser and Gly. Intramolecular rebinding of NO, O_2, and methyl isocyanide to Arg^{45}, Ser^{45}, Glu^{45}, and Lys^{45}(native) pig myoglobins was measured following 35-ps and 17-ns excitation pulses. The shorter, picosecond laser flash was used to examine ligand recombination from photochemically produced contact pairs, and the longer, nanosecond flash was used to measure the rebinding of ligands farther removed from the iron atom. Mutations at position 45 or esterification of the heme did not change significantly (≤2-fold) the overall association rate constants for NO, CO, and O_2 binding at room temperature. These data demonstrate unequivocally that Lys(Arg)^{45} makes little contribution to the outer kinetic barrier for the entry of diatomic gases into the distal pocket of myoglobin, a result that contradicts a variety of previous structural and theoretical interpretations. However, the rates of geminate recombination of NO and O_2 and the affinity of myoglobin for O_2 were dependent upon the basicity of residue 45. The series of substitutions Arg^{45}, Lys^{45}, Ser^{45}, and Glu^{45} in pig myoglobin led to a 3-fold decrease in the initial rate for the intramolecular, picosecond rebinding of NO and a 4-fold decrease in the geminate rate constant for the nanosecond rebinding of O_2. The Arg^{45} to Glu substitution also caused a 4-fold decrease in the O_2 affinity of pig myoglobin, which was due primarily to an increase in the overall oxygen dissociation rate constant. These results show that both the stability of the liganded, six-coordinate state and the geminate reactivity of unliganded, five-coordinate deoxymyoglobin are influenced by residue 45. The replacement of residue 45 with a polar or negatively charged amino acid caused substantial increases in the overall association rate constants for the binding of alkyl isocyanides. Elimination of the Arg^{45}–propionate interactions by reconstitution of sperm whale myoglobin with protoheme IX dimethyl ester also enhanced the rate of alkyl isocyanide binding. These results suggest that the salt bridge between Arg^{45} or Lys^{45} and the heme-6-propionate does inhibit the movement of the larger isocyanide ligands into the distal pocket, presumably by restricting the motions of His^{64}.

The X-ray structures of O_2 and CO sperm whale myoglobin have revealed much about the significance of amino acid residues near the ligand binding site. However, the role of these residues in ligand movement into the active site is not well-understood even though myoglobin is viewed as a model system for studying and simulating the motions of small molecules in protein matrices. Early molecular dynamics calculations suggested that ligands enter and exit the heme pocket through a pathway between Val^{68}(E11) and His^{64}(E7) (Case & Karplus, 1979; Kottalam & Case, 1988). This channel requires passage through the solvent-exposed side of the heme pocket, which includes residue 45(CD3) and the heme-6-propionate. Almost all mammalian myoglobins have lysine at residue 45; the exceptions are sperm whale and aardvark myoglobins which have arginine at this position.[1] In sperm whale oxymyoglobin, the guanidino portion of the side chain of Arg^{45}(CD3) lies between His^{64} and external solvent (Figure 1); Lys^{45}(CD3) occupies a similar position in pig

† This research was supported by U.S. Public Health Service Grants GM-35649 (J.S.O.), GM-14276 (Q.H.G.), GM-33775 (S.G.S.), and GM-31756 (S.G.S.), Grant GR/E 98867 (A.J.W.) from the Science and Engineering Research Council, U.K., Grant C-612 (J.S.O.) from the Robert A. Welch Foundation, and Grant 4073 (J.S.O.) from the Advanced Technology Program of the Texas Higher Education Coordinating Board. T.E.C. is a recipient of a graduate fellowship from the National Institutes of Health, Training Grant GM-07933 from the National Institute of Medical Science.

[1] A listing of known mammalian myoglobin sequences was obtained by using the EuGene & SAM software package developed by the Molecular Biology Information Resource, Department of Cell Biology, Baylor College of Medicine, Houston, TX, and the Protein Sequence Data Bank from the National Biomedical Research Foundation, Washington, DC.

0006-2960/91/0430-4697$02.50/0

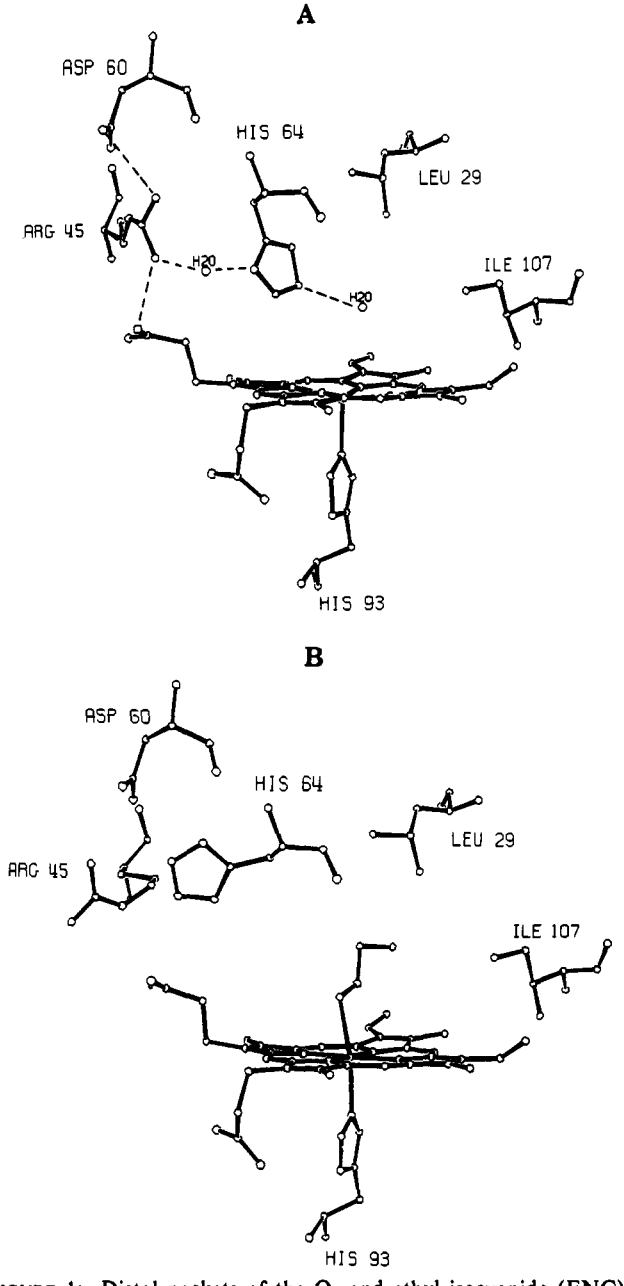

FIGURE 1: Distal pockets of the O_2 and ethyl isocyanide (ENC) complexes of sperm whale myoglobin. The coordinates for panel A were taken from the structure of MbO_2 determined by Phillips (1980). The coordinates for panel B were taken from the "open" conformation of the MbENC structure determined by Johnson et al. (1989). The ORTEP drawings were generated from a side view starting from outside the protein, looking through the E-helix toward the CD corner.

myoglobin (Smerdon et al., 1990). The electrostatic and polar interactions involving these groups and surface water molecules have been postulated to be part of the barrier to ligand entry into the heme pocket (Lecomte & La Mar, 1985). La Mar and co-workers have also suggested that residue 45 and the heme-6-propionate form a salt bridge which increases the affinity of apomyoglobin for hemin and orients the binding of the prosthetic group (La Mar et al., 1986).

X-ray structures of sperm whale myoglobin containing bulky ligands suggest that His^{64} may serve as a gate restricting access to the iron atom (Figure 1). Structures of imidazole and phenylhydrazine complexes of metmyoglobin show rotation of His^{64} out of the heme pocket and movement of Arg^{45} into the solvent phase (Bolognesi et al., 1982; Ringe et al., 1984). In the structure of ethyl isocyanide sperm whale myoglobin, His^{64} is not rigidly fixed and occupies the displaced position only 45% of the time while Arg^{45} lies in the outer solvent position 75% of the time (Figure 1B; Johnson et al., 1989). Even in CO sperm whale myoglobin, His^{64} moves slightly relative to its position in the deoxy structure, and the Arg^{45}-(CD3) side chain rotates toward the interior of the protein about 50% of the time (Kuriyan et al., 1986). This flexibility provides evidence that Arg^{45}, moving in tandem with His^{64}, may influence the opening and closing of a passage to the iron atom.

Lecomte and La Mar (1985) suggested that residue 45, together with Asp^{60} and the heme-6-propionate, is part of a triad of electrostatic interactions which stabilize the "closed door" position of His^{64} (Figure 1). More recently, Elber (1990) carried out molecular dynamics simulations of O_2 escape from the distal pockets of native and mutant sperm whale myoglobins. For the Arg^{45}(native) protein, little or no O_2 escaped through the His^{64} gate pathway in 1.6 ns after thermal dissociation. This calculation led Elber and Karplus (1990) to suggest that O_2 enters and leaves native myoglobin by alternative pathways between the E- and G-helices. In contrast, when Gly was present at position 45, roughly 25% of the O_2 molecules had escaped through the His^{64} pathway in 800 ps. Thus, these theoretical computations also suggest that the basic residue at the CD3 position in myoglobin is part of a major kinetic barrier to ligand entry into and exit from the heme pocket.

We have tested these ideas by measuring overall kinetic parameters for the binding of O_2, CO, and methyl, ethyl, *n*-propyl, and *n*-butyl isocyanide to pig myoglobin containing Arg^{45}, Lys^{45}(native), His^{45}, Ser^{45}, or Glu^{45} and to sperm whale myoglobin containing Arg^{45}(native), Ser^{45}, Gly^{45}, or protoheme IX dimethyl ester. His^{45} and Ser^{45} pig myoglobins were synthesized to mimic the CD3 residue in human α and β chains, respectively; Gly^{45} and Glu^{45} myoglobins were made to examine the importance of size and charge at position 45. Sperm whale myoglobin was reconstituted with protoheme dimethyl ester to eliminate the electrostatic interactions between the heme-6-propionate and Arg^{45}. Since ligand migration from solvent into the protein is rate-limiting for alkyl isocyanide binding, the overall association rate constants for the binding of these larger ligands are sensitive to changes in the accessibility of the heme pocket (Gibson et al., 1986). Laser photolysis techniques were used to measure geminate recombination parameters for NO, O_2, and methyl isocyanide binding to Lys^{45}(native), Arg^{45}, Ser^{45}, and Glu^{45} pig myoglobin at room temperature.

Lambright et al. (1989) examined the effects of the Lys^{45} to Arg substitution on the overall rate constants for CO binding to human myoglobin, and our results for CO binding to pig myoglobin are in agreement with their observations. These workers also examined the effects of mutating Asp^{60} to Glu on CO binding, since residue 60 appears to interact electrostatically with Arg^{45} in sperm whale myoglobin. We have measured the effects of replacing Asp^{60} with Ser on the binding of six different ligands to pig myoglobin.

Experimental Procedures

Preparation of Proteins and Samples for Measurements. Native sperm whale myoglobin (type II) and protohemin IX were obtained from Sigma Chemical Co. prior to the ban on whale products. A detailed description of the mutagenesis of sperm whale myoglobin is given by Westrick et al. (1990). Briefly, the *PstI–KpnI* fragment of pMb413a [synthetic sperm whale myoglobin (Springer & Sligar, 1987)] was subcloned into M13mp19 (New England Biolabs). All subsequent ma-

nipulations were performed according to the method of Taylor et al. (1985), utilizing the Amersham oligonucleotide-directed in vitro mutagenesis system. Mutant oligonucleotides were synthesized at the Genetic Engineering Facility, University of Illinois, Urbana, IL. Mutations were selected by the loss of a *Pvu*I site and were identified by DNA sequencing as described by Sanger et al. (1977). The mutant genes were subcloned back into pUC19 for subsequent expression in *Escherichia coli* strain TB-1 (Bethesda Research Laboratories).

The subcloning and expression of recombinant pig myoglobin in *E. coli* have been described (Dodson et al., 1988). For mutagenesis, a 600 base pair *Bam*HI/*Hin*dIII fragment isolated from M13mp11FXpmyo was ligated to similarly digested pBluescript-KS$^+$ DNA (Stratagene Inc.) to produce pSJS1008. Single-stranded DNA was prepared from pSJS1008-transformed DH5αF'(F', ϕ80*dlac*ZM15,Δ(*lac*Z-YA-*arg*F)U169, *rec*A1, *end*A1, *hsd*R17, *sup*E44, λ^-,*thi*-1, *gyr*A96, *rel*A1) following inoculation of shaking cultures with helper phage R408 (Stratagene Inc.) at a multiplicity of infection of 20. Mutagenesis reactions and colony screening were performed as described by Zoller and Smith (1984) using oligonucleotides containing one or more mismatches. Putative mutant clones were confirmed by DNA sequencing of the entire myoglobin coding region (Sanger et al., 1977). Expression and purification of wild-type and mutant pig myoglobins were carried out by using the pLcII system as described previously (Dodson et al., 1988; Nagai & Thøgersen, 1984).

Protohemin IX dimethyl ester was synthesized as part of a reaction generating both the mono- and dimethyl esters of the hemin. The pivalyl dianhydride of protohemin was prepared in a septum-sealed flask flushed with N_2 as described in Traylor et al. (1979). Ten milliliters of 65% MeOH in H_2O was added to the anhydride solution to yield a mixture of the diester, monoacid monoester, and diacid forms of protohemin. The crude product was dried, dissolved in chloroform, and washed with 1% HCl. The sample was then purified on a 4 × 40 cm silica gel column packed and eluted with 9:1:0.01 $CHCl_3$/MeOH/Et_3N. The dimethyl ester eluted first, followed by the monoacid and diacid derivatives. Fractions containing pure dimethyl ester were identified by silica gel thin-layer chromatography in 85:15 $CHCl_3$/MeOH (R_f = 0.7), pooled, and dried in a rotary evaporator. The sample was then resuspended in $CHCl_3$ washed 2× with 1% HCl, 1× with 1% Na_2CO_3, and 3× with H_2O. Sperm whale apomyoglobin was prepared by extraction with 2-butanone according to Teale (1959). Myoglobin was reconstituted with dicyano dimethyl ester protohemin IX according to the method outlined in La Mar et al. (1986) for the incorporation of substituted hemes. As a control, apomyoglobin was also reconstituted with protohemin IX by the same method to form the normal holoprotein; this protein was found to have spectral and kinetic properties identical with those of native sperm whale myoglobin (Light et al., 1987). After several days, the reconstituted myoglobin was checked for hydrolysis of the ester groups by extraction with 2-butanone and TLC of the hemin. The cyano derivative of ferric protoheme dimethyl ester sperm whale myoglobin was relatively unstable. Repeated freeze–thawing or storage at 4 °C for longer than several days led to precipitation of protein and loss of heme. Consequently, fresh preparations were used without freezing and thawing whenever possible.

Rapid Mixing and Conventional Photolysis Experiments. Association and dissociation rate constants were measured by stopped-flow rapid mixing and conventional flash photolysis techniques as described in detail by Rohlfs et al. (1990). Association equilibrium constants were calculated as the ratio of the rate constants. Under pseudo-first-order conditions, all of the pig and sperm whale myoglobin mutants and derivatives exhibited monophasic, exponential time courses. For most proteins, the absence of kinetic heterogeneity was demonstrated by measuring rate constants with both a rapid mixing and a conventional flash photolysis apparatus, and identical results were obtained in both types of experiment. Some time courses for the binding of large isonitriles to the protoheme dimethyl ester derivative of sperm whale myoglobin did show a small slow component which comprised less than 10% of the total absorbance change. Wild-type sperm whale myoglobin expressed in *E. coli* has previously been shown to be identical in tertiary structure and function with native sperm whale myoglobin (Rohlfs et al., 1990; Phillips et al., 1990). Pig myoglobin expressed in *E. coli* also exhibits ligand binding properties indistinguishable from those of the native protein (Table I).

Nanosecond and Picosecond Photolysis Experiments. Tonometers equipped with 1-mm path length cuvettes were used for the NO, O_2, and CO reactions. Alkyl isocyanide complexes were prepared in 1-mm path length cuvettes sealed with a serum stopper as described in Gibson et al. (1986). The myoglobin concentrations were 20–100 μM in 0.1 M potassium phosphate, pH 7.0, 20 °C. For the measurement of time courses with half-times greater than 10 ns, a Phase-R 2100B dye laser was used to generate rectangular 17-ns pulses in cavity-dump mode with a switching time of less than 2 ns. Data were collected with a Hamamatsu photomultiplier attached to a Tektronix Model 7104 oscilloscope interfaced to an IBM AT computer (Carver et al., 1990). For the faster picosecond reactions, a Nd-YAG active–passive mode-locked laser (Quantel Model YG571) was used to generate 35-ps pulses at 1064 nm that were frequency doubled to 532 nm. Pulse–probe data collection was performed as described in Carver et al. (1990).

Results

NO, O_2, and CO Binding. Association and dissociation rate constants for O_2, CO, and methyl, ethyl, *n*-propyl, and *n*-butyl isocyanide binding to pig and sperm whale derivatives are given in Tables I and II. Native pig and sperm whale myoglobins showed similar ligand binding parameters, which is not surprising since these proteins differ at only 21 out of 153 amino acid positions. Mutation of Lys^{45} to His, Ser, and Glu in pig myoglobin produced no effect on the overall association rate constants for NO, CO, or O_2 binding (Tables I and III). In contrast, the Lys^{45} to Arg mutation caused a 2-fold increase in the CO association rate (Table I) analogous to that observed for the same substitution in human myoglobin (Lambright et al., 1989). Mutation of Arg^{45} to Ser and Gly in sperm whale myoglobin resulted in small (≤2-fold) decreases in the association rate constants for O_2 and CO binding, and similar effects were observed for the protoheme dimethyl ester derivative of the native protein (Table II and Figure 2B). The Asp^{60} to Ser mutation had no effect on any of the ligand binding properties of pig myoglobin (Table I). Lambright et al. (1989) also reported no effect on CO binding for the more conservative Asp^{60} to Glu mutation in human myoglobin.

The effects of residue 45 mutation and heme modification on the association equilibrium constants for ligand binding are shown in Figure 2. Arg^{45} pig myoglobin has a 2–3-fold higher affinity for both O_2 and CO than the Lys^{45}(native) protein (Figure 2A). Lambright et al. (1989) also reported an increase in CO affinity when Arg was substituted for Lys^{45} in human

Table I: Overall Rate and Equilibrium Constants for Ligand Binding to Native and Mutant Pig Myoglobins[a]

ligand	pig myoglobin mutant	k' (μM^{-1} s^{-1})	k (s^{-1})	K (μM^{-1})
O_2	Lys^{45}(native)	17	14	1.2
	Lys^{45}(*E. coli*)	18	14	1.3
	His^{45}	17	31	0.53
	Arg^{45}	21	8.1	2.5
	Ser^{45}	19	26	0.72
	Glu^{45}	18	30	0.62
	Ser^{60}	17	11	1.5
CO	Lys^{45}(native)	0.78	0.019	41
	Lys^{45}(*E. coli*)	0.73	0.019	38
	His^{45}	0.73	0.024	30
	Arg^{45}	1.5	0.014	110
	Ser^{45}	0.72	0.019	38
	Glu^{45}	0.76	0.030	25
	Ser^{60}	0.92	0.019	48
MNC	Lys^{45}(native)	0.11	4.4	0.025
	Lys^{45}(*E. coli*)	0.11	4.4	0.025
	His^{45}	0.11	4.7	0.024
	Arg^{45}	0.10	2.7	0.038
	Ser^{45}	0.16	4.4	0.037
	Glu^{45}	0.23	4.7	0.049
	Ser^{60}	0.10	4.0	0.025
ENC	Lys^{45}(native)	0.098	0.63	0.15
	Lys^{45}(*E. coli*)	0.098	0.63	0.15
	His^{45}	0.11	0.61	0.17
	Arg^{45}	0.083	0.33	0.25
	Ser^{45}	0.19	1.0	0.19
	Glu^{45}	0.29	1.0	0.28
	Ser^{60}	0.097	0.53	0.18
*n*PNC	Lys^{45}(native)	0.059	0.70	0.084
	Lys^{45}(*E. coli*)	0.063	0.70	0.090
	His^{45}	0.078	0.58	0.13
	Arg^{45}	0.052	0.57	0.091
	Ser^{45}	0.13	0.72	0.19
	Glu^{45}	0.23	0.46	0.51
	Ser^{60}	0.062	0.65	0.095
*n*BNC	Lys^{45}(native)	0.040	0.50	0.079
	Lys^{45}(*E. coli*)	0.040	0.50	0.081
	His^{45}	0.057	0.49	0.12
	Arg^{45}	0.040	0.55	0.073
	Ser^{45}	0.081	0.46	0.18
	Glu^{45}	0.18	0.36	0.51
	Ser^{60}	0.037	0.50	0.073

[a] 0.1 M potassium phosphate at 20 °C, pH 7.0. Rate constants were generally measured for only 1–2 protein preparations; hence standard deviations could not be computed. On the basis of identical measurements with sperm whale myoglobin (Table II), a relative error of ±20% is assumed to apply to the parameters measured for pig myoglobin. The alkyl isocyanide abbreviations are as follows: MNC, methyl; ENC, ethyl; *n*PNC, *n*-propyl; and *n*BNC, *n*-butyl.

myoglobin. The O_2 and CO association equilibrium constants for the other pig mutants decreased slightly compared to those for native or wild-type myoglobin (Figure 2A). Significantly larger decreases in O_2 and CO affinity were observed when Arg^{45} was replaced with Ser or Gly in sperm whale myoglobin (Figure 2B).

Alkyl Isocyanide Binding. The association rate constants for alkyl isocyanide binding to both pig and sperm whale mutants display a consistent pattern. Substituting a polar or negatively charged residue for $Lys(Arg)^{45}$ led to significant increases in the association rate constants for methyl, ethyl, *n*-propyl, and *n*-butyl isocyanide binding to pig and sperm whale myoglobins (Tables I and II). In general, the magnitude of this effect increases with the length of the alkyl side chain of the isocyanide.

The association equilibrium constants for methyl and ethyl isocyanide binding to pig myoglobin increased in the order Lys^{45}(native) ≈ His^{45} < Ser^{45} ≈ Arg^{45} < Glu^{45}. For *n*-propyl and *n*-butyl isocyanide binding, the order of affinities was Lys^{45}(native) ≈ Arg^{45} < His^{45} < Ser^{45} < Glu^{45} (Figure 2A).

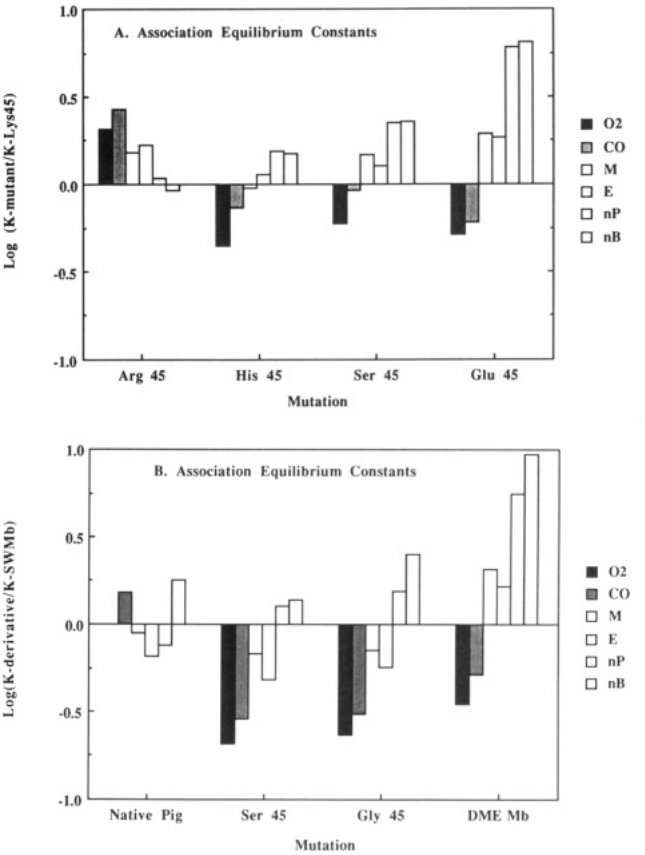

FIGURE 2: (A) Dependence of the association equilibrium constant (K) on the size and basicity of the 45(CD3) amino acid in pig myoglobin. Logarithms of the ratio of K for a given mutant to that for native (Lys^{45}) myoglobin were calculated for O_2, CO, and methyl (M), ethyl (E), *n*-propyl (nP), and *n*-butyl (nB) isocyanide binding to the Arg^{45}, His^{45}, Ser^{45}, and Glu^{45} mutants. The legend in the figure going from top (O_2) to bottom (nB) refers to the bars going from left (solid bar) to right (open bar) for each protein. (B) Effects of removal of the Arg^{45}–heme-6-propionate salt bridge on the association equilibrium constant (K) for ligand binding to sperm whale myoglobin. Logarithms for the ratio of K for a given protein to that for native (Arg^{45}) sperm whale myoglobin were calculated for O_2, CO, and methyl (M), ethyl (E), *n*-propyl (nP), and *n*-butyl (nB) isocyanide binding to native (Lys^{45}) pig myoglobin and Ser^{45}, Gly^{45}, and dimethyl ester protoheme substituted sperm whale myoglobin. The legend and bar symbols are the same as those in panel A.

For the Ser^{45} and Gly^{45} mutants of sperm whale myoglobin, the methyl and ethyl isocyanide affinities decreased compared to those for the native Arg^{45}(native) protein, whereas the *n*-propyl and *n*-butyl isocyanide affinities increased (Figure 2B). The most pronounced effect was a 10-fold increase in the affinity constant for *n*-butyl isocyanide binding to the protoheme dimethyl ester derivative of sperm whale myoglobin, which corresponds to a −1.3 kcal/mol change in the free energy of binding (Table II). However, for this derivative, we have no information regarding either the degree of orientational disorder of the dimethyl ester heme or the effects of the loss of the His^{97}–heme-7-propionate linkage; these factors could contribute to the more favorable binding of large ligands (Light et al., 1987).

Picosecond NO Rebinding to Pig Myoglobins. The quantum yield of geminate states was low (0.1–0.2) for both the O_2 and NO complexes of pig myoglobin even when a 35-ps excitation pulse was used (Q_{ps} values in Table III). The quantum yields for the generation of photodissociated CO and methyl isocyanide intermediates were much larger and approached 1.0. The O_2, CO, and methyl isocyanide complexes of native pig myoglobin and the position 45 mutants showed

Table II: Overall Rate and Equilibrium Constants for Ligand Binding to Native and Substituted Sperm Whale Myoglobins[a]

ligand	sperm whale myoglobin derivative	k' (μM^{-1} s^{-1})	k (s^{-1})	K (μM^{-1})
O_2	Arg^{45}(native)	14 ± 3	12 ± 2	1.2 ± 0.3
	Ser^{45}	8.0	31	0.25
	Gly^{45}	6.8	24	0.28
	DME	8.0	19	0.42
CO	Arg^{45}(native)	0.51 ± 0.06	0.019 ± 0.005	27 ± 8
	Ser^{45}	0.29	0.037	7.8
	Gly^{45}	0.33	0.040	8.3
	DME	0.39	0.027	14
MNC	Arg^{45}(native)	0.12 ± 0.02	4.3 ± 0.3	0.028 ± 0.006
	Ser^{45}	0.15	7.7	0.019
	Gly^{45}	0.17	8.3	0.020
	DME	0.19	3.3	0.058
ENC	Arg^{45}(native)	0.069 ± 0.01	0.30 ± 0.03	0.23 ± 0.05
	Ser^{45}	0.15	1.4	0.11
	Gly^{45}	0.16	1.2	0.13
	DME	0.17	0.43	0.38
*n*PNC	Arg^{45}(native)	0.042 ± 0.01	0.39 ± 0.02	0.11 ± 0.03
	Ser^{45}	0.11	0.77	0.14
	Gly^{45}	0.12	0.72	0.17
	DME	0.19	0.31	0.61
*n*BNC	Arg^{45}(native)	0.030 ± 0.002	0.69 ± 0.05	0.044 ± 0.004
	Ser^{45}	0.034	0.56	0.061
	Gly^{45}	0.066	0.61	0.11
	DME	0.12	0.29	0.41

[a] 0.1 M potassium phosphate at 20 °C, pH 7.0. The errors for native myoglobin were determined as the standard deviation from the mean of at least 7 completely independent determinations with different protein samples over the past 7 years (Mims et al., 1983; Rohlfs et al., 1990). For the other sperm whale derivatives, rate constants were generally measured for only 1–2 protein preparations, and as a result, standard deviations could not be computed. The relative errors for native myoglobin are assumed to apply to parameters for the other proteins (i.e., ±20%). The alkyl isocyanide abbreviations are as follows: MNC, methyl; ENC, ethyl; *n*PNC, *n*-propyl; and *n*BNC, *n*-butyl. Another abbreviation used: DME, sperm whale myoglobin reconstituted with protoheme IX dimethyl ester.

no geminate recombination on picosecond time scales.[2] In contrast, NO rebinding was extremely rapid, with greater than 95% recombination occurring in less than 1 ns after photolysis (Figure 3A). All of these results are qualitatively similar to those reported by Carver et al. (1990) for the corresponding liganded complexes of sperm whale myoglobin.

As was the case for sperm whale protein, the geminate recombination time courses for the NO complexes of pig myoglobin were heterogeneous and could be fitted equally well to sequential or parallel reaction schemes of the type:

$$A \rightleftharpoons B_1 \rightleftharpoons B_2 \quad \text{or} \quad \begin{matrix} A_1 \rightleftharpoons B_1 \\ \| \\ A_2 \rightleftharpoons B_2 \end{matrix} \qquad (1)$$

where A, A_1, and A_2 represent equilibrium bound states. The B states are interpreted as iron–ligand contact pairs in which the photodissociated NO is within one or two van der Waals radii of the iron atom (Jongeward et al., 1988). In the linear mechanism, multiple intermediates are generated by sequential movements of the ligand away from the iron atom; in the parallel mechanism, the different geminate states result from either multiple ground-state conformations or the decay of a common photoexcited species into two different geminate states (Doster et al., 1982; Petrich et al., 1988; Jongeward et al., 1988; Carver et al., 1990). To be consistent with our previous work with sperm whale myoglobin, the NO recombination time courses for the position 45 mutants were fitted to the sequential scheme by integrating the corresponding differential equations both during and after the 35-ps excitation pulse as described

Table III: Kinetic Parameters for NO Rebinding to Native and Mutant Pig Myoglobins[a]

mutant	overall k' (μM^{-1} s^{-1})	picosecond geminate recombination parameters: k_{B_1A} (ns^{-1})	$k_{B_1B_2}$ (ns^{-1})	$k_{B_2B_1}$ (ns^{-1})	Q_{ps}
Arg^{45}	16	24	5	6	0.25
Lys^{45}	17	14 ± 3	5 ● 2	3 ± 1	0.20 ± 0.03
Ser^{45}	16	10	3	2	0.22
Glu^{45}	16	7.4	3	1	0.16

[a] 0.1 M potassium phosphate at 20 °C, pH 7.0. Picosecond recombination time courses were fitted to the linear consecutive reaction scheme by numerically integrating the rate expressions in eq 1 as described in the text. Alternative analyses could have been made with a parallel reaction scheme. For example, the data for Lys^{45}(native) pig myoglobin can be fitted equally well as two independent kinetic phases: 73% of the absorbance change with a rate equal to 1.9×10^{10} s^{-1} and the remaining 27% with a rate equal to 2.2×10^9 s^{-1}. Thus, the fitted parameters shown above should be viewed as an empirical description of the observed time courses. The errors for the native (Lys^{45}) parameters were calculated as the standard deviation from the mean of 3 independent determinations. The other values represent single determinations.

[2] The lack of picosecond recombination reactions for these ligands conflicts with the results of Jongeward et al. (1988), who reported measurable 20–50-ps relaxations for the O_2, methyl isocyanide, ethyl isocyanide, and *tert*-butyl isocyanide complexes of native sperm whale myoglobin following a 0.07-ps excitation pulse. However, the spectral changes shown for their MbO_2^* samples indicated that complex photophysical processes were occurring. In particular, a short-lived ($\tau \leq 12$ ps), long-wavelength intermediate (λ_{max} = 450–470 nm) intermediate is apparent in their difference spectra and was not resolved from the geminate recombination changes. Petrich et al. (1988) also observed a short-lived photoexcited state (τ = 3 ps), but these workers, like us (Carver et al., 1990), were unable to observe any longer lived, geminate picosecond intermediates for native MbO_2 samples at room temperature. In unpublished work, we have measured large picosecond intermediates for *tert*-butyl isocyanide rebinding to native sperm whale myoglobin; however, none could be detected for the smaller isocyanides. We have also shown that the overall quantum yields for the methyl and ethyl isocyanide complexes of native sperm whale myoglobin are identical, within ±10%, with the corresponding fractions of ligand escape to the solvent from the nanosecond intermediate [$k_{CX}/(k_{CA} + k_{CX})$, eq 2]. This independent experimental observation suggests strongly that there are no additional faster geminate recombination steps for the native sperm whale myoglobin complexes of these ligands [see Carver et al. (1990) and references therein].

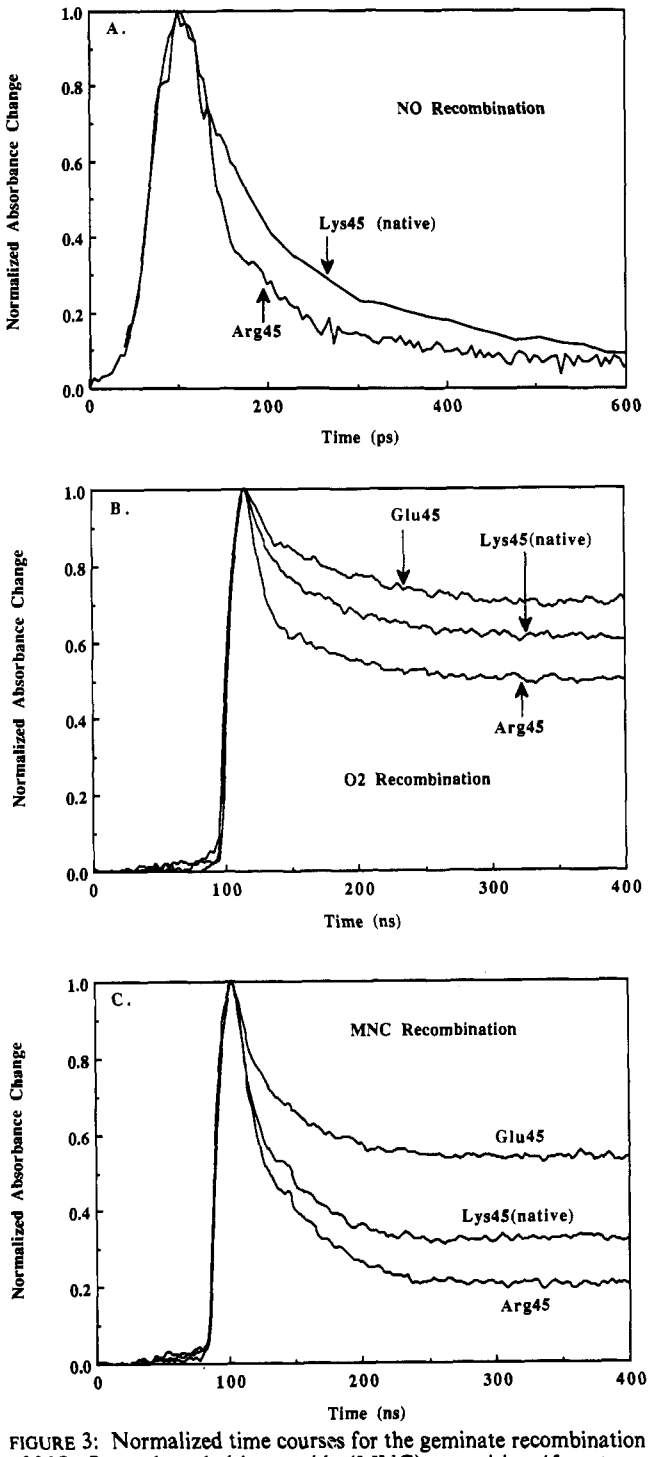

FIGURE 3: Normalized time courses for the geminate recombination of NO, O_2, and methyl isocyanide (MNC) to position 45 mutants of pig myoglobin. Conditions: 20–100 μM myoglobin in 0.1 M potassium phosphate, pH 7.0, 20 °C. The solid lines connect observed data points. (A) Time courses for picosecond rebinding of nitric oxide to myoglobin mutants monitored at 436 nm during and after a 35-ps light pulse. (B) Time courses for nanosecond rebinding of O_2 to pig myoglobin mutants, monitored at 436 nm during and after an attenuated 17-ns light pulse. (C) Time courses for nanosecond rebinding of MNC to myoglobin mutants monitored at 445 nm during and after an attenuated 17-ns light pulse.

by Carver et al. (1990). The fitted parameters are given in Table III, where Q_{ps} is the quantum yield for the formation of state B_1, k_{B_1A} is the rate of iron–ligand bond formation from state B_1, and $k_{B_1B_2}$ and $k_{B_2B_1}$ are the rates of interconversion of the two sequential B states.

Regardless of the exact mechanistic interpretation, the results in Table III show that the positive charge on the native residue at position 45 does affect the initial rate of geminate NO recombination. The k_{B_1A} value for Arg^{45} pig myoglobin was 3 times greater than that for the Glu^{45} mutant, and this trend extended to the slower kinetic phase since $k_{B_2B_1}$ also decreased when Glu was substituted for Arg^{45}.

Nanosecond O_2 and Methyl Isocyanide Rebinding to Pig Myoglobins. Geminate recombination phases were observed on nanosecond time scales for the O_2 and methyl isocyanide complexes of native pig myoglobin and the position 45 mutants (Figure 3 and Table IV). Unfortunately, we were unable to measure geminate CO rebinding to these proteins using the 17-ns laser photolysis apparatus because the extent of recombination was small (≤5–10%) and obscured by the breakthrough of laser light before and after cavity dumping [see Carver et al. (1990)].

The nanosecond time courses observed for the O_2 and methyl isocyanide derivatives are thought to represent rebinding by ligand molecules farther removed from the iron and bound noncovalently in the distal portion of the heme pocket. These intermediates have been designated C to distinguish them from the more rapidly recombining contact pairs or B states (Jongeward et al., 1988; Chatfield et al., 1990; Carver et al., 1990). Most workers assume a consecutive scheme for interconnecting the geminate picosecond, geminate nanosecond, and bimolecular millisecond reactions (i.e., A ⇌ B ⇌ C ⇌ Mb + X, where Mb + X represents deoxymyoglobin plus ligand free in solution). The lack of measurable picosecond intermediates (B states) for the O_2 and methyl isocyanide complexes is interpreted as due to the low reactivities of these ligands in the contact pair compared to the rate of movement into state C (i.e., $k_{BA} \ll k_{BC}$).[2] Consequently, only one geminate recombination phase is observed and can usually be analyzed by a simple two-step consecutive reaction scheme [see Carver et al. (1990)]:

$$\mathrm{MbX\ or\ A} \underset{k_{h\nu}Q_{ns}I(t)+k_{AC}}{\overset{k_{CA}}{\rightleftharpoons}} \mathrm{C} \underset{k_{CX}}{\overset{k'_{XC}}{\rightleftharpoons}} \mathrm{X + Mb} \qquad (2)$$

After the flash pulse, the observed first-order rate constant is given by $k_{CA} + k_{CX}$, where k_{CA} is the unimolecular rate constant for formation of the iron–ligand bond starting with ligand in state C and k_{CX} is the rate constant for ligand escape from the distal pocket into the solvent phase. $k_{h\nu}Q_{ns}I(t)$ represents the rate of photodissociation of the ligand complex during the excitation pulse. $I(t)$ is relative light intensity of the beam at time t; Q_{ns} is the quantum yield for the formation of state C; and $k_{h\nu}$ is a proportionality constant determined empirically with CO myoglobin as a standard [see Carver et al. (1990)]. k'_{XC} is the bimolecular rate constant for ligand movement into the protein, and k_{AC} is the unimolecular rate constant for thermal disruption of the iron–ligand bond.

Sets of nanosecond time courses were collected at different laser light intensities and then analyzed in terms of eq 2 by integrating the rate equations for states A and C both during and after the 17-ns flash pulse as described by Carver et al. (1990). Fitted parameters for O_2 and methyl isocyanide rebinding to Arg^{45}, Lys^{45}(native), Ser^{45}, and Glu^{45} pig myoglobin are shown in Table IV. Values for k'_{XC} and k_{AC} were computed from the overall association (k') and dissociation (k) rate constants by using the formulas: $k'_{XC} = k'(k_{CA} + k_{CX})/k_{CA}$ and $k_{AC} = k(k_{CA} + k_{CX})/k_{CX}$.

The fitted rate parameters for O_2 rebinding to pig myoglobin are similar to those reported previously for other mammalian myoglobins (Jongeward et al., 1988; Sato et al., 1990; Chatfield et al., 1990; Carver et al., 1990). About 50% of the photodissociated O_2 molecules recombined with the native protein at a rate equal to 3×10^7 s^{-1}, which is roughly 70%

Table IV: Kinetic Parameters for O_2 and Methyl Isocyanide Rebinding to Position 45(CD3) Mutants of Pig Myoglobin[a]

ligand	mutant	k'_{XC} ($\mu M^{-1} s^{-1}$)	k_{CX} (μs^{-1})	K_{XC} (M^{-1})	k_{CA} (μs^{-1})	k_{AC} (s^{-1})	K_{AC} ($\times 10^{-6}$)	Q_{ns}
O_2	Arg^{45}	31	21	1.5	42	24	1.8	0.14
	Lys^{45}(native)	33	15	2.2	17	30	0.57	0.19
	Ser^{45}	39	15	2.7	13	43	0.30	0.16
	Glu^{45}	44	16	2.7	11	46	0.25	0.14
MNC	Arg^{45}	0.12	5.0	0.023	33	20	1.6	(1.0)
	Lys^{45}(native)	0.14	9.4	0.015	33	20	1.6	(1.0)
	Ser^{45}	0.26	18	0.014	32	12	2.6	(1.0)
	Glu^{45}	0.40	15	0.026	22	12	1.9	(1.0)

[a] 0.1 M potassium phosphate at 20 °C, pH 7.0. Symbols are from eq 2. All experiments with the mutants were carried out at least twice. Error analyses of similar data for sperm whale myoglobin gave standard deviations of ±20–30% for the values of k'_{Xc}, k_{Cx}, and k_{CA} and ±40–60% for K_{XC}, k_{AC}, and K_{AC} (Carver et al., 1990).

greater than that observed for sperm whale myoglobin at pH 7, 20 °C. All the time courses fitted well to a simple two-step scheme at 20 °C, but it is important to note that heterogeneous O_2 recombination time courses have been reported at lower temperatures (Chatfield et al., 1990) and at room temperature for other myoglobin mutants (Carver et al., 1990). The largest effect of mutagenesis at position 45 was a 2–3-fold increase in the intramolecular rate of bond formation when Lys^{45} was replaced by Arg. This increase in k_{CA} relative to k_{CX} caused an increase in both the rate and extent of O_2 recombination (Figure 3B).

The time courses for methyl isocyanide recombination to the pig myoglobins were also monophasic, similar to those of sperm whale myoglobin, and were readily analyzed in terms of eq 2. k_{CA} for this ligand was little affected by mutagenesis at position 45, but the rate constants for entry into and escape from the protein, k'_{XC} and k_{CX}, increased 3–4-fold for the series $Arg^{45} < Lys^{45} < Ser^{45} < Glu^{45}$ pig myoglobin (Table IV). Phenomenologically, the net result was similar to that observed for the O_2 complexes: the Arg^{45} mutant showed the greatest extent of geminate recombination, and the Glu^{45} mutant, the least (Figure 3C).

Discussion

Comparison of Effects in Pig and Sperm Whale Myoglobins. Most mammalian myoglobins show similar reactivities toward ligands (Goss et al., 1982), a behavior predictable from their homologous sequences. Thus, we anticipated that mutation of the same residue in different myoglobins would produce the same functional results. However, the data in Tables I and II and Figure 2 initially suggested that alteration of residue 45 caused different effects in pig and sperm whale myoglobins. The Arg^{45} to Ser substitution in sperm whale myoglobin led to 4–5-fold decreases in CO and O_2 affinities, whereas the Lys^{45} to Ser substitution in pig myoglobin caused only small decreases in the protein's affinities for these ligands. This apparent discrepancy is due in part to differences between the native residues, Lys^{45} in pig and Arg^{45} in sperm whale myoglobin. Even though the positive charge of residue 45 is preserved, the Lys^{45} to Arg substitution in pig myoglobin is less conservative functionally than the Lys^{45} to Ser mutation and produces a protein with O_2 and CO affinities significantly greater than those of sperm whale myoglobin. Similar results have been reported for CO binding to the Arg^{45} mutant of human myoglobin (Lambright et al., 1989).

The relative effects of the artificial Arg^{45} to Ser mutation on the equilibrium binding constants for pig myoglobin are very similar to those observed for the same substitution in sperm whale myoglobin (Figure 4). Thus, residue 45 is likely to be in a similar environment in both proteins. These results also show that site-directed mutagenesis in either myoglobin could be used to determine the functional role of residue 45.

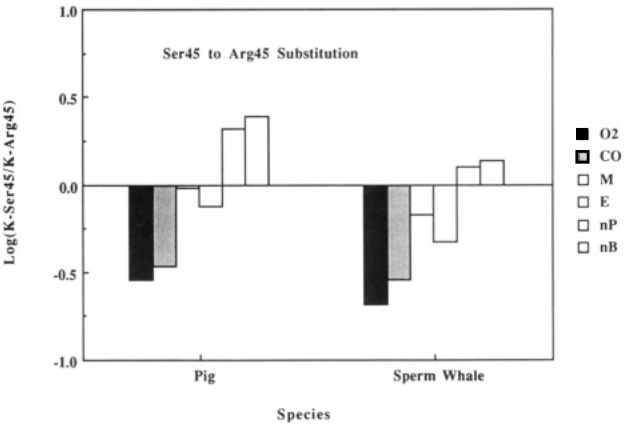

FIGURE 4: Comparison of association equilibrium constants for the Arg^{45} to Ser mutation in pig and sperm whale myoglobins. Logarithms of the ratio of K for Ser^{45} to that for Arg^{45} myoglobin were calculated for O_2, CO, methyl (M), ethyl (E), *n*-propyl (nP), and *n*-butyl (nB) isocyanide binding to the pig and sperm whale proteins. The legend in the figure going from top (O_2) to bottom (nB) refers to the bars going from left (solid bar) to right (open bar) for each protein.

However, even though the Arg^{45} to Ser mutation produces the same relative effects, Ser^{45} pig and Ser^{45} sperm whale myoglobins differ significantly in their absolute reactivities toward ligands. For example, Ser^{45} pig myoglobin has ligand affinities that are consistently 2–3-fold greater than those for its sperm whale counterpart (Tables I and II). Thus, in native pig myoglobin, subtle differences elsewhere in the protein raise the reactivity of the iron atom, compensating for the absence of an arginine at position 45. The net result is nearly identical rate and equilibrium constants for O_2 and CO binding to native pig and sperm whale myoglobins. These compensating differences probably occur in most mammalian myoglobins containing Lys^{45} in their native sequences since Arg^{45} human myoglobin also has increased overall CO association rate and equilibrium constants which are close to those for Arg^{45} pig myoglobin (Lambright et al., 1989).

Structure of the Distal Pocket and Physiological Significance. The proximity of the CD corner to the distal pocket in myoglobin suggests that residue 45(CD3) may be involved in orienting key distal amino acids located along the E-helix. Residue 45 may interact directly or through water molecules with His^{64} and Thr^{67}. The residue 45–heme-propionate salt bridge may also serve to bring the heme ring into closer contact with the side chains of His^{64}, Val^{68}, and Phe^{43} (Figure 1). Disruption of the salt bridge should result in a more flexible heme pocket structure which, in turn, may alter the contacts between the bound ligand and adjacent distal residues. The affinities of heme proteins for alkyl isocyanides have been shown to be strongly affected by steric hindrance between the bound ligand and distal residues (Mims et al., 1983; Rohlfs

et al., 1990). A profile of these effects based on ligand size can be established by measuring the equilibrium constants for the binding of the n-series of alkyl isocyanides. For both pig and sperm whale myoglobins, these profiles suggest that replacement of the basic side chain at position 45 with a polar or acidic group results in reduced steric hindrance of large ligands (Figure 2). For example, the Lys^{45} to Glu mutation caused a 6-fold increase in the affinity of pig myoglobin for *n*-butyl isocyanide (Table I). Similar increases in isocyanide affinities were obtained for sperm whale myoglobin reconstituted with protoheme dimethyl ester (Figure 2B).

These structural perturbations have physiological significance. His^{45}, Ser^{45}, and Glu^{45} pig myoglobin and sperm whale myoglobin containing Ser^{45}, Gly^{45}, and protoheme dimethyl ester all showed 2–4-fold reductions in oxygen affinity relative to native myoglobin (Tables I, II, and IV). The 4-fold decrease in K_{O_2} for the series Arg^{45}, Lys^{45}, His^{45}, Ser^{45}, and Gly^{45} to Glu^{45} was mainly the result of increases in the O_2 dissociation rate constant. Two possible explanations for the increase in k_{O_2} are the following: (1) a weakening of the His^{64}–O_2 interaction due to increases in the freedom of movement of the imidazole group and/or decreases in its hydrogen bond donor character and (2) decreases in the stability of the Fe–O_2 bond due to proximal effects mediated by the residue 45–heme-6-propionate interaction (Figure 1A). Our current results cannot distinguish between these possibilities.

Effects on the Inner and Outer Kinetic Barriers. Little perturbation of the intramolecular dynamics of oxygen binding to pig myoglobin occurred when Lys^{45} was replaced with either a Glu or a Ser (Table IV). In contrast, the Lys^{45} to Arg mutation increased the rate constant for recombination from state C (k_{CA} in eq 2). These results may explain why this mutation had only a small effect on the overall O_2 association rate constant but increased the CO association rate constant 2-fold. The outer kinetic barrier for entry into myoglobin and the inner barrier for rebinding from within the distal pocket are believed to be about the same height for O_2 and to make roughly equal contributions to the overall association rate constant (Carver et al., 1990). Thus, small changes in the inner kinetic barrier or the stability of state C do not cause large changes in the overall association rate constant for O_2 binding. In contrast, the inner kinetic barrier for CO binding is much larger than the outer barrier, and alterations that affect either the inner barrier or the stability of state C lead directly to changes in the CO association rate constant. Expressed mathematically, the overall association rate constant for CO is defined as the product of the equilibrium constant for the formation of state C, K_{XC}, and the rate constant for iron–ligand bond formation, k_{CA} (Doster et al., 1982; Gibson et al., 1986; Jongeward et al., 1988). For the Lys^{45} to Arg substitution in pig myoglobin, K_{XC} was decreased only 30% for O_2 binding whereas k_{CA} increased 3-fold. If these relative changes also apply to CO binding, the overall CO association rate constant should increase 2-fold as was observed (Table I). The more rapid picosecond rebinding of NO to the Arg^{45} mutant [and to native Arg^{45} sperm whale myoglobin; see Carver et al. (1990)] compared to native pig myoglobin also indicates a lowering of the innermost kinetic barrier for iron–ligand bond formation compared to that of the native Lys^{45} protein (Table III). Thus, increasing the basicity of residue 45 increases the reactivity of the iron atom, causing greater rates of geminate rebinding, lower rates of oxygen dissociation, and a net increase in O_2 affinity.

A small increase in the bimolecular rate constant for O_2 entry into the protein was observed with decreasing basicity of the residue 45 side chain (k'_{XC} values in Table IV); however, these differences are within the range of estimated experimental error. This dependence was more pronounced for methyl isocyanide binding. The Lys^{45} to Glu substitution in pig myoglobin caused 3–4-fold increases in both k'_{XC} and k_{CX}, suggesting a 1 kcal/mol reduction in the outer kinetic barrier for methyl isocyanide binding. This decrease in resistance to ligand movement into the protein accounts for the larger association rate constants observed for alkyl isocyanide binding to the Glu^{45} mutant (Table I).

Pathways for Ligand Binding. Although Case and Karplus (1979) and later Kottalam and Case (1988) proposed that the major pathway for ligand entry into and exit from the heme pocket may lie between His^{64} and Val^{68}, more recent molecular dynamics calculations suggest that additional escape routes may be available for ligand dissociation from myoglobin (Elber & Karplus, 1990; Elber, 1990). Unfortunately, the latter calculations could only be performed in vacuo. A rigorous evaluation of the contribution of side-chain interactions to ligand trajectories, particularly those involving residue 45 (CD3), requires simulating water molecules in exposed regions of the protein. Regardless of which pathway predominates, the X-ray structures of liganded sperm whale myoglobin indicate that polar and electrostatic interactions at the heme periphery involving residue 45 and the heme-6-propionate should affect movements of the imidazole side chain of His^{64} and of the E-helix as a whole (Ringe et al., 1985; Johnson et al., 1989). These motions certainly appear to be required to open a direct channel to the distal pocket (Perutz, 1989; Figure 1). However, as shown in Tables I and II, rather drastic substitutions at position 45 in myoglobin produced little effect on the association rate constants for O_2, CO, and NO binding. This experimental result contradicts the structural interpretations described above which predicted that the salt bridge between residue 45 and the heme-6-propionate should block formation of the channel for O_2 movement into and out of myoglobin.

Arg^{45} and Lys^{45} do inhibit the entry of large ligands into the protein since the Gly^{45}, Ser^{45}, and Glu^{45} mutants all showed increased overall association rate constants for isocyanide binding compared to those for native or wild-type myoglobin. This discrimination based on ligand size indicates that either (1) the smaller diatomic ligands follow a different route to gain access to the iron atom as suggested by Elber and Karplus (1990) or (2) all ligands follow the same pathway, but entry of the larger isocyanide ligands is more restricted, requires larger movements of the His^{64} side chain, and is, therefore, more sensitive to changes in the polar interactions at the heme periphery. Although the first possibility cannot be ruled out, the second explanation appears more likely, based on results which show that certain position 64 and 68 mutations in sperm whale myoglobin affect the outer kinetic barriers for both diatomic and isocyanide ligands (Egeberg et al., 1990; Carver et al., 1990), on the X-ray data for large ligand complexes (Bolognesi et al., 1982; Ringe et al., 1984; Johnson et al., 1989), and on photoacoustic calorimetry studies of CO photodissociation (Westrick et al., 1990).

Conclusions. Since the $Lys(Arg)^{45}$ residue is completely conserved in mammalian myoglobins, it could have an important structural or physiological function. The results in Tables I and II and Figures 2–4 show that decreasing the basicity and altering the charge of residue 45 decreases the association equilibrium constant for oxygen binding to myoglobin. Thus, residue 45 does regulate the oxygen affinity of myoglobin, although to a far lesser extent than His^{64} (Springer

et al., 1989; Rohlfs et al., 1990). Other functions of residue 45 may include aiding the binding of heme to apomyoglobin by electrostatic interactions with the heme-6-propionate (La Mar et al., 1986) and interacting with components of a metmyoglobin reductase system. Gacon et al. (1980) have shown that positively charged surface residues in the vicinity of the heme pocket appear to play a role in the interaction of human hemoglobin subunits with the erythrocyte reduction system. Our results show that residue 45 could participate in these interactions without greatly affecting the rate of entry of diatomic ligands into the distal pocket.

Registry No. O_2, 7782-44-7; CO, 630-08-0; MeNCO, 593-75-9; EtNCO, 624-79-3; PrNCO, 627-36-1; BuNCO, 2769-64-4; Arg, 74-79-3; Lys, 56-87-1.

REFERENCES

Bolognesi, M., Cannillo, E., Ascenzi, P., Giacometti, G. M., Merli, A., & Brunori, M. (1982) *J. Mol. Biol. 158*, 305–315.

Carver, T. E., Rohlfs, R. J., Olson, J. S., Gibson, Q. H., Blackmore, R. J., Springer, B. A., & Sligar, S. G. (1990) *J. Biol. Chem. 265*, 20007–20020.

Case, P. A., & Karplus, M. (1979) *J. Mol. Biol. 132*, 343–368.

Chatfield, M. D., Walda, K. N., & Magde, D. (1990) *J. Am. Chem. Soc. 112*, 4680–4687.

Dodson, G. G., Hubbard, R. E., Oldfield, T. J., Smerdon, S. J., & Wilkinson, A. J. (1988) *Protein Eng. 2*, 233–237.

Doster, W., Beece, D., Bowne, S. F., DiIorio, E. E., Eisenstein, L., Frauenfelder, H., Reinisch, L., Shyamsunder, E., Winterhalter, K. H., & Yue, K. T. (1982) *Biochemistry 21*, 4831–4839.

Egeberg, K. D., Springer, B. A., Sligar, S. G., Carver, T. E., Rohlfs, R. J., & Olson, J. S. (1990) *J. Biol. Chem. 265*, 11788–11795.

Elber, R. (1990) Simulation of Ligand Diffusion in Myoglobin and Myoglobin Mutants, in *Research Summaries for Forgarty Internal Center Conference on the Dynamics and Kinetics of Myoglobin and Hemoglobin* (Brunori, M., Eaton, W. A., Gibson, Q. H., & Karplus, M., Eds.) June 25–27, p 23, National Institutes of Health, Bethesda, MD.

Elber, R., & Karplus, M. (1990) *J. Am. Chem. Soc. 112*, 9161–9175.

Gacon, G., Lostanlen, D., Labie, D., & Kaplan, J.-C. (1980) *Proc. Natl. Acad. Sci. U.S.A. 77*, 1917–1921.

Gibson, Q. H., Olson, J. S., McKinnie, R. E., & Rohlfs, R. J. (1986) *J. Biol. Chem. 261*, 10228–10239.

Goss, D. J., LaGow, J. B., & Parkhurst, L. J. (1982) *Comp. Biochem. Physiol. 71*, 229–233.

Johnson, K. A., Olson, J. S., & Phillips, G. N. (1989) *J. Mol. Biol. 207*, 459–463.

Jongeward, K. A., Magde, D., Taube, D. J., Marsters, J. C., Traylor, T. G., & Sharma, V. S. (1988) *J. Am. Chem. Soc. 110*, 380–387.

Kottalam, J., & Case, D. A. (1988) *J. Am. Chem. Soc. 110*, 7690–7697.

Kuriyan, J., Wilz, S., Karplus, M., & Petsko, G. A. (1986) *J. Mol. Biol. 192*, 133–154.

La Mar, G. N., Emerson, D., Lecomte, J. T. J., Pande, U., Smith, K. M., Craig, G. W., & Kehres, L. A. (1986) *J. Am. Chem. Soc. 108*, 5568–5573.

Lambright, D. G., Balasubramian, S., & Boxer, S. G. (1989) *J. Mol. Biol. 207*, 289–299.

Lecomte, T. J., & La Mar, G. N. (1985) *Biochemistry 24*, 7388–7395.

Light, R. W., Rohlfs, R. J., Palmer, G., & Olson, J. S. (1987) *J. Biol. Chem. 262*, 46–52.

Mims, M. P., Porras, A. G., Olson, J. S., Noble, R. W., & Peterson, J. A. (1983) *J. Biol. Chem. 258*, 14219–14232.

Nagai, K., & Thøgersen, H.-C. (1984) *Nature 309*, 810–812.

Perutz, M. F. (1989) *Trends Biochem. Sci. 14*, 42–44.

Petrich, J. W., Poyart, C., & Martin, J. L. (1988) *Biochemistry 27*, 4049–4060.

Phillips, G. N., Arduini, R. M., Springer, B. A., & Sligar, S. G. (1990) *Proteins 7*, 358–365.

Phillips, S. E. V. (1980) *J. Mol. Biol. 142*, 531–554.

Ringe, D., Petsko, G. A., Kerr, D., & Ortiz de Montellano, P. R. (1984) *Biochemistry 23*, 2–4.

Rohlfs, R. J., Mathews, A. J., Carver, T. E., Olson, J. S., Springer, B. A., Egeberg, K. D., & Sligar, S. G. (1990) *J. Biol. Chem. 265*, 3168–3176.

Sanger, F., Nicklen, S., & Coulson, A. R. (1977) *Proc. Natl. Acad. Sci. U.S.A. 74*, 5463–5467.

Sato, F., Shiro, Y., Sokaguchi, Y., Izuka, T., & Hayashi, H. (1990) *J. Biol. Chem. 265*, 18823–18828.

Smerdon, S. J., Oldfield, T. J., Dodson, E. J., Dodson, G. G., Hubbard, R. E., & Wilkinson, A. J. (1990) *Acta Crystallogr. B46*, 370–377.

Springer, B. A., & Sligar, S. G. (1987) *Proc. Natl. Acad. Sci. U.S.A. 84*, 8961–8965.

Springer, B. A., Egeberg, K. D., Sligar, S. G., Rohlfs, R. J., Mathews, A. J., & Olson, J. S. (1989) *J. Biol. Chem. 264*, 3057–3060.

Taylor, J. W., Ott, J., & Eckstein, F. (1985) *Nucleic Acids Res. 13*, 8764–8785.

Teale, F. W. J. (1959) *Biochim. Biophys. Acta 35*, 543.

Traylor, T. G., Chang, C. K., Geibel, J., Berzinis, A., Mincey, T., & Cannon, J. (1979) *J. Am. Chem. Soc. 101*, 6716–6731.

Westrick, J. A., Peters, K. S., Ropp, J. D., & Sligar, S. G. (1990) *Biochemistry 29*, 6741–6746.

Zoller, M. J., & Smith, M. (1984) *DNA 3*, 479–488.